

# Pair Spectrometer Hodoscope for Hall D at Jefferson Lab<sup>☆</sup>

F.Barbosa<sup>a</sup>, C.Hutton<sup>a</sup>, A.Sitnikov<sup>a</sup>, A.Somov<sup>a,\*</sup>, S.Somov<sup>b</sup>, I.Tolstukhin<sup>b</sup>

<sup>a</sup>Thomas Jefferson National Accelerator Facility, Newport News, VA 23606, USA

<sup>b</sup>National Research Nuclear University MEPhI, Moscow, Russia

---

## Abstract

We present the design of the pair spectrometer hodoscope fabricated at Jefferson Lab and installed in the experimental Hall D. The hodoscope consists of thin scintillator tiles; the light from each tile is collected using wave-length shifting fibers and detected using a Hamamatsu silicon photomultiplier. Light collection was measured using relativistic electrons produced in the tagger area of the experimental Hall B.

*Keywords:* Scintillator detector, Pair spectrometer, Silicon photomultiplier

---

## 1. Introduction

2 The new detector GlueX has been constructed in the experimental Hall D at Thomas  
3 Jefferson National Accelerator Facility. The main physics goal of the GlueX experi-  
4 ment [1] is to search for hybrid mesons with exotic quantum numbers using a beam  
5 of linearly polarized photons incident on a liquid hydrogen target. The linearly polar-  
6 ized photon beam in Hall D will be produced via the coherent bremsstrahlung process  
7 by 12 GeV electrons in a thin diamond radiator. Coherent bremsstrahlung has been  
8 successfully used to produce linearly polarized photon beams at various experimen-  
9 tal facilities [2, 3]. Coherent radiation from a diamond crystal lattice results in sharp  
10 monochromatic peaks in the photon energy spectrum. The peak energy depends on  
11 the relative orientation of the electron beam direction and the crystal lattice, and can

---

<sup>☆</sup>Notice: Authored by Jefferson Science Associates, LLC under U.S. DOE Contract No. DE-AC05-06OR23177. The U.S. Government retains a non-exclusive, paid-up, irrevocable, world-wide license to publish or reproduce this manuscript for U.S. Government purposes.

\*Corresponding author. Tel.: +1 757 269 5553; fax: +1 757 269 6331.

Email address: somov@jlab.org (A.Somov)

12 be adjusted in the experiment by rotating the diamond. The GlueX photon energy re-  
13 gion of interest corresponding to the main coherent peak is between 8.4 GeV and 9.1  
14 GeV. The fraction of linearly polarized photons can be increased by passing a pho-  
15 ton beam through a 3.4 mm diameter collimator situated about 75 m downstream of  
16 the radiator. The collimator preferentially filters out photons produced via incoherent  
17 bremsstrahlung, which have a substantially larger mean emission angle. The colli-  
18 mated photons propagate toward the GlueX target. The energy of a beam photon can  
19 be inferred by analyzing the momentum of the electron after it has radiated the pho-  
20 ton, given that the primary beam energy is known. This so-called “tagged” electron is  
21 deflected in a 6 m long dipole magnet operated at a field of 1.8 T and is subsequently  
22 registered in the tagging microscope or broad-band hodoscope scintillator counters.

23 One of the key components of the Hall D photon beam line is the magnetic pair  
24 spectrometer, which is installed after the photon collimator in front of the GlueX de-  
25 tector. The spectrometer will reconstruct the energy of a beam photon by detecting  
26 the  $e^\pm$  pair produced by the photon in a thin converter. The main purpose of the spec-  
27 trometer is to measure the spectrum of the collimated photon beam and determine the  
28 fraction of linearly polarized photons in the coherent peak energy region. It will also  
29 monitor the photon beam flux and can be used for the energy calibration of the tagging  
30 hodoscope and microscope detectors. The description of the Hall D pair spectrometer  
31 will be presented in Section 2. The design of the pair spectrometer high-granularity  
32 hodoscope and light collection measurements from hodoscope scintillator tiles will be  
33 described in Section 3 and Section 4, respectively.

## 34 **2. Pair Spectrometer**

35 Layout of the Hall D pair spectrometer is presented in Fig. 1. Electron-positron  
36 pairs are created by beam photons inside a thin converter with a typical thickness rang-  
37 ing between  $10^{-4} - 10^{-2}$  radiation lengths. The choice of the converter thickness de-  
38 pends on the photon beam flux. The maximum flux for GlueX physics runs is expected  
39 to be  $5 \cdot 10^7$   $\gamma$ /sec in the coherent peak energy region. Three converters with different  
40 thicknesses are installed in a movable fork, that can insert one of them into the photon

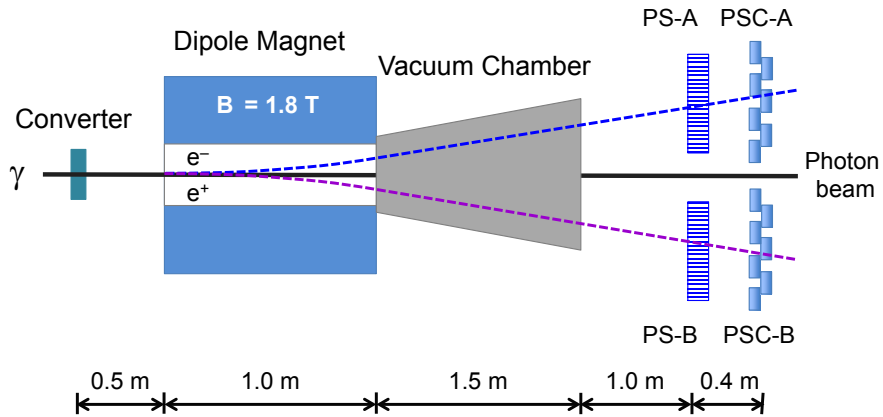


Figure 1: Schematic top view of the Hall D pair spectrometer. PS and PSC denote the hodoscope and coarse scintillator counters, respectively.

41 beam. Produced leptons are deflected in a 18D36 dipole magnet with an effective field  
 42 length of about 0.94 m. The magnet was brought from Brookhaven National Labora-  
 43 tory and was modified at Jefferson Lab by reducing the pole gap from 6 inches to 3  
 44 inches. The magnet is operated at a nominal field of 1.8 T. A 1.5 meter long vacuum  
 45 chamber is installed after the magnet. Electrons and positrons are registered in two  
 46 layers of scintillator detectors: a high-granularity hodoscope and a set of coarse coun-  
 47 ters, denoted in Fig. 1 as PS and PSC, respectively. The detectors are organized into  
 48 two arms positioned symmetrically with respect to the photon beam line. Each detector  
 49 arm covers a momentum range of  $e^\pm$  between 3.0 GeV/c to 6.2 GeV/c, correspond-  
 50 ing to reconstructed photon energies between 6 GeV and 12.4 GeV. Relatively large accep-  
 51 tance of the hodoscope allows one to reconstruct photons with energies in the coherent  
 52 peak energy region and also in the range near the beam end-point energy of 12 GeV.  
 53 This can be used for the energy calibration of the hodoscope detectors.

54 The high-resolution hodoscope is used for precise measurements of  $e^\pm$  momenta.  
 55 The hodoscope consists of a set of thin scintillator tiles, stacked together. Momentum  
 56 of the reconstructed lepton is related to the  $x$ -coordinate of each tile, where  $x$  is an axis  
 57 perpendicular to the beam line. Hodoscope tiles will be calibrated in units of lepton

58 energy, the energy scale will be used hereafter in the text. The hodoscope momen-  
59 tum resolution was studied using a detailed Geant detector simulation. The hodoscope  
60 energy resolution varies between 12 MeV and 20 MeV for 6 GeV and 12 GeV re-  
61 constructed photons, respectively. Light from each scintillator tile is detected using a  
62 Hamamatsu silicon photomultiplier (SiPM). The detailed description of the hodoscope  
63 will be presented in Section 3.

64 Sixteen coarse scintillator counters, eight in each detector arm, are positioned about  
65 40 cm behind the hodoscope. The counters are 4.4 cm wide in the direction perpen-  
66 dicular to the lepton trajectory, 2 cm thick, and 6 cm in height. Hamamatsu R6427-01  
67 PMTs are used to detect the scintillation light. The counters are used to produce a pair  
68 spectrometer trigger by requiring a coincidence of hits in the two detector arms. They  
69 also help to reduce background originating from interactions of  $e^\pm$  inside the magnet  
70 pole edges to the level below 1% by constraining  $e^\pm$  trajectories. Counter rates depend  
71 on the converter thickness and photon beam flux. The maximum rate will not exceed  
72 10 kHz per PSC counter during GlueX operation.

73 Signals from both the hodoscope and coarse counters are digitized using a twelve-  
74 bit multi-channel flash ADC operated at a sampling rate of 250 MHz [5]. The PSC  
75 counters are also instrumented with TDCs, with a channel width of 60 ps [6]. The  
76 time resolution is expected to be better than 200 ps. This resolution will allow one to  
77 distinguish the electron beam bunch where the bremsstrahlung photon is emitted and  
78 therefore relate hits from the pair spectrometer and tagging detectors originating from  
79 the same event.

### 80 **3. Pair Spectrometer Hodoscope**

#### 81 *3.1. Design and Fabrication*

82 The pair spectrometer hodoscope consists of 145 rectangular tiles made of EJ-212  
83 scintillator [4], stacked together as shown in Fig. 2. The tile height is 3 cm and the  
84 length along the electron path in scintillator is 1 cm. Tiles with two different widths,  
85 in the direction perpendicular to the electron trajectory, of 2 mm and 1 mm are used.  
86 Forty 1 mm wide tiles are instrumented in the detector high-energy region around 6

87 GeV in order to provide better energy resolution in this energy range. The energy bin  
88 size of the hodoscope tiles varies depending on the lepton energy and constitutes about  
89 13 MeV and 24 MeV for 3 GeV and 6 GeV leptons, respectively. Tiles are optically  
90 isolated using 10  $\mu\text{m}$  aluminized Mylar foil. This reflective foil also covers the bottom  
91 of the tile assembly. The deflection angle of leptons in the dipole magnet depends on  
92 the lepton momentum; the angular spread is about 5 degrees between 3 GeV and 6.2  
93 GeV electrons. To account for the angular dependence, hodoscope tiles are organized  
94 into 18 groups. Each group is tilted by about 0.3 degrees. This was done by attaching a  
95 shim, a  $\sim 50 \mu\text{m}$  thick adhesive strip, to one side of the aluminum foil after each group.

96 Light from a tile is collected using two 20 cm long 1 mm x 1 mm square double-  
97 clad BCF-92 wave-length shifting (WLS) fibers, each of which is glued to the side of  
98 the tile using BC 600 Optical Cement. A tile assembly with two WLS optical fibers  
99 is shown in Fig. 3. The peak of the emission spectrum for EJ-212 scintillator occurs  
100 at the wavelength of 423 nm, which couples well with the absorption spectrum of the  
101 BCF-92 fiber. Light is subsequently reemitted inside the fiber in the green range with  
102 an emission peak of 492 nm.

103 Collected light is transmitted to the end of the WLS fiber. A pair of fibers from each  
104 tile is inserted into a hole in an aluminum mounting plate, as shown on the upper plot  
105 of Fig. 2. An electronics circuit board containing 145 photo detectors is attached to  
106 the mounting plate. Each photo sensor is coupled to two WLS fibers from a single tile.  
107 The light detection is performed using Hamamatsu surface mount S10931-050P silicon  
108 photomultipliers with an effective photosensitive area of 3 mm x 3 mm and a pixel size  
109 of 50  $\mu\text{m}$ . These sensors have a photon detection efficiency (PDE) larger than 20% at  
110 a wavelength of 500 nm and a typical gain of about  $7 \cdot 10^5$  [7]. The electronics board  
111 with SiPMs is presented in Fig. 4. The SiPMs are arranged in two arrays of 3 x 35 and  
112 5 x 8 sensors, which are connected to 2 mm and 1 mm tiles, respectively. SiPMs are  
113 optically isolated using a plastic spacer.

### 114 3.2. *Electronics*

115 The hodoscope front end electronics consists of an amplifier and a SiPM bias volt-  
116 age control circuit developed at Jefferson Lab. Signals from the SiPMs are amplified

117 using the amplifier with a gain of about a factor of 20. The amplifier is based on  
118 commercially available devices (operational amplifiers) with 3 GHz bandwidth. Pulse  
119 shaping is employed to compensate for the characteristically high SiPM capacitance  
120 and package inductance. The impulse response shows rise and fall times of 3 ns and  
121 with trans-impedance gain of 1 mV/ $\mu$ A. The SiPM operating bias voltage is about 73  
122 V. The nominal bias setting is as specified by Hamamatsu (1 V over voltage) and fed  
123 to the SiPM through a resistive network employing a thermistor and a linearizing resis-  
124 tor. The hodoscope control electronics supply individually adjusted voltages to groups  
125 of 5 SiPM channels; inside the group the voltage is adjusted among channels using  
126 resistors. The thermistor senses the average temperature of closely packed SiPMs in  
127 thermal equilibrium via a heat spreader PCB layout, thus forming a well controlled  
128 loop. The commercially available bias power supply has very low noise characteris-  
129 tics and is well regulated to less than 1 mV long term. The supply allows the user to  
130 monitor and adjust the levels as needed and if required. The optimal bias setting will  
131 be determined based on experimental conditions. Amplified SiPM signals are digitized  
132 by flash ADCs positioned in two readout VXS crates. An example of the flash ADC  
133 signal pulse obtained from a scintillator tile is shown in Fig. 5. The ADC sampling  
134 time is 4 ns.

135 After fabrication, the performance of SiPMs and electronics were tested using a  
136 picoseconds laser light pulser<sup>1</sup>. The typical rise time of a SiPM pulse produced by a  
137 laser pulser is about 6 ns and the corresponding fall time is 45 ns. The pulser trigger  
138 output was used to initiate the flash ADC readout. SiPM amplitudes digitized by ADC  
139 are integrated in a time window of 60 ns. A typical ADC spectrum is shown in Fig. 6.  
140 Peaks on this plot correspond to the number of pixels fired in the SiPM. The position  
141 of a single-pixel peak depends on the combined gain of a SiPM and electronics. The  
142 single-pixel peak distribution measured for all hodoscope SiPMs is presented in Fig. 7.  
143 The solid curve corresponds to the fit of this distribution to a Gaussian function. The  
144 relative gain variation is found to be smaller than 1.5%.

---

<sup>1</sup>Hamamatsu PLP-10 light pulser was used to test the hodoscope electronics.

## 145 **4. Light Collection Studies**

### 146 *4.1. Beam Test*

147 During the design phase of the hodoscope, we studied light collection from scin-  
148 tillator tiles using a detector prototype that consisted of fourteen 2 cm x 1 cm x 1 mm  
149 and five 2 cm x 1 cm x 2 mm tiles. Tiles were made from the same scintillator type  
150 EJ-212 but had smaller height of 2 cm. Light collection was performed using a sin-  
151 gle BCF-92 fiber, which was glued to one side of the tile using DYMAX UV optical  
152 adhesive. Light was detected by Hamamatsu SiPMs S10362-11-025C and S10362-11-  
153 050C, which have the pixel size of 25  $\mu\text{m}$  and 50  $\mu\text{m}$ , respectively. These SiPMs have  
154 a smaller sensitive area of 1 mm x 1 mm. Prototypes of the SiPM amplifier and the  
155 bias control circuit were used. The trigger was provided by a small plastic scintillator  
156 mounted behind the tiles. The trigger scintillator was connected to a Philips XP 1911  
157 photomultiplier tube via two optical fibers. The setup used in the beam test is shown in  
158 Fig. 8. SiPM pulses were digitized using a flash ADC in a VXS crate.

159 The hodoscope prototype was positioned in the tagger area of the experimental Hall  
160 B at Jefferson Lab [3] and was operated concurrently with the CLAS detector. The  
161 CLAS used a secondary beam of photons produced in the tagger area by the Jefferson  
162 Lab electron beam in a thin radiator via the bremsstrahlung process. A beam electron  
163 that radiates a photon is deflected in the dipole tagger magnet and sent to the floor of  
164 the experimental hall. The prototype was placed inside a light-tight box and positioned  
165 on the floor of the tagger area. The hodoscope was oriented in such a way that it  
166 faced normal to the path of electrons, i.e., electrons travel 1 cm through the tile. A  
167 schematic view of the tagger area and the location of the prototype is shown in Fig. 9.  
168 Dashed curves on this plot denote trajectories of tagged electrons with the fractional  
169 energy  $k/E_0$ , where  $k$  is the tagged electron energy and  $E_0$  is the electron beam energy.  
170 Data was taken with an electron beam energy of 2.54 GeV, corresponding to a tagged  
171 electron energy of about 1.4 GeV.

The amount of light collected from a tile was measured in units of pixels fired in  
the SiPM. The average number of pixels was estimated to be

$$N_{\text{pixels}} = A_{\text{peak}}/A_{\text{single}}, \quad (1)$$

172 where  $A_{\text{peak}}$  is the ADC value corresponding to the maximum of an ADC spectrum  
173 measured in the beam test and  $A_{\text{single}}$  is the ADC value of a single pixel peak. The  
174 position of the single pixel peak was calibrated using a LED pulser. Exact counting  
175 of the number of photons that induce pixel-breakdowns is complicated due to the op-  
176 tical cross-talk and after-pulses in the SiPM. The cross-talk is produced by secondary  
177 photons emitted in the pixel breakdown that trigger an additional avalanche in a neigh-  
178 boring pixel. The after-pulsing is believed to be produced by charge carriers that are  
179 released from the substrate after some delay from the avalanche resulting in consec-  
180 utive SiPM pulses. The cross-talk and after-pulse probabilities for the SiPMs used in  
181 the hodoscope are expected to be relatively small, less than 10% [8]. For the prototype  
182 operational bias voltage (about 1 V over) we expect on average about 0.2 pixels fire  
183 per incident photon. SiPM operational voltages for the final detector will be adjusted  
184 according to the experimental conditions and detector performance.

185 The beam test results are listed in Table 1. The amount of light collected from the  
186 1 mm and 2 mm wide tiles is found to be almost the same and corresponds to about  
187 29 pixels fired in the SiPM with the pixel size of 50  $\mu\text{m}$ . This indicates that the light  
188 collection mainly depends on the surface of the WLS fiber glued to the tile, which is  
189 similar for 1 mm and 2 mm tiles. The fewer number of fired pixels measured with a  
190 25  $\mu\text{m}$  SiPM is consistent with about a factor of two smaller photon detection efficiency  
191 of these SiPMs compared with 50  $\mu\text{m}$  SiPMs. The smaller pixel fill factor (the ratio of  
192 the active area of a pixel to the entire area) accounts for the smaller PDE for the 25  $\mu\text{m}$   
193 S10362-11-025C SiPMs. We estimate that errors on light collection measurements are  
194 dominated by alignment of the WLS fiber with respect to the SiPM. The sensitive area  
195 of SiPMs used in the prototype is the same as the fiber cross section.

196 Light collection from the final hodoscope detector will be performed using two  
197 WLS fibers and SiPMs with a factor of 9 larger effective area. Therefore, we expect  
198 about a factor of two more light collected from the tile and a SiPM response corre-  
199 sponding to about 60 fired pixels. This amount of light should be sufficient to provide a  
200 high detection efficiency for  $e^{\pm}$  pairs in the hodoscope. The hodoscope can be operated  
201 at relatively small ADC thresholds because a coincidence of hits in two detector arms



Tile width (mm)	1		2
SiPM pixel size ( $\mu\text{m}$ )	25	50	50
Light detected (pixels)	$16.1 \pm 2.1$	$28.7 \pm 3.4$	$29.2 \pm 3.6$

Table 1: The amount of light in units of fired pixels seen by SiPM for various tiles used in the beam test.

202 is required.

#### 203 4.2. Cosmic Setup

204 During the fabrication of scintillator tiles for the final hodoscope, we checked light  
205 collection using a cosmic ray setup presented in Fig. 10. Muon candidates were se-  
206 lected using two small trigger scintillator counters with an effective area of 6 mm x  
207 3 cm and thickness of 2 mm. Counters were positioned perpendicular to each other  
208 and formed an overlap region of 6 mm x 6 mm. The distance between scintillators  
209 was about 20 cm. A hodoscope tile was placed between these counters, in such a way  
210 that cosmic particles go perpendicular to the tile, in the middle. The average muon  
211 path length in the scintillator corresponds to the tile width. A lead brick about 10 cm  
212 thick was position above the bottom scintillator to filter low-energy particles. Light  
213 detection was performed using a Hamamatsu S10931-050P SiPM instrumented with a  
214 single-channel amplifier. The amplifier gain was about a factor of ten smaller than that  
215 used in the hodoscope. A typical ADC spectrum obtained from the SiPM is shown on  
216 the top plot of Fig. 11. The average amount of light collected from 2 mm wide tiles  
217 corresponds to about 18 pixels fired in the SiPM. A Sr90 source was used to check  
218 quality of some selected fabricated tile assemblies. The SiPM spectrum obtained from  
219 a 2 mm wide tile using the radioactive source is shown on the bottom plot of Fig. 11  
220 for comparison.

### 221 5. Summary

222 We have described the design and fabrication details of the pair spectrometer ho-  
223 doscope, an array of thin scintillator tiles. Light from each tile is detected using a 3

224 mm x 3 mm Hamamatsu SiPM. A detector prototype was built to perform light collec-  
225 tion studies using relativistic electrons produced in the experimental Hall B at Jefferson  
226 Lab. The amount of light for 1 mm and 2 mm tiles measured with the prototype corre-  
227 sponds to a SiPM response of about 29 fired pixels. At least a factor of two more light  
228 is expected for the final hodoscope for which the light collection is performed using  
229 two WLS fibers and tiles with larger size, i.e., larger light collection surface, are used.  
230 This amount of light is sufficient to provide a high detection efficiency of leptons by  
231 the hodoscope. Two arms of the hodoscope detector were commissioned and installed  
232 in the experimental Hall D.

## 233 **6. Acknowledgments**

234 This work was supported by the Department of Energy. Jefferson Science Asso-  
235 ciates, LLC operated Thomas Jefferson National Accelerator Facility for the United  
236 States Department of Energy under contract DE-AC05-06OR23177. We would like to  
237 thank the CLAS Collaboration for an opportunity to conduct the beam test at Hall B  
238 and especially Eugene Pasyuk and Sergey Boyarinov for the assistance with the beam  
239 test. We are also thankful to Slava Razmyslovich for his help with preparing some  
240 technical drawings for the hodoscope.

## 241 **References**

- 242 [1] JLab Experiment E12-06-102, (2006) [http://www.jlab.org/exp\\_prog/  
243 proposals/06/PR12-06-102.pdf](http://www.jlab.org/exp_prog/proposals/06/PR12-06-102.pdf).
- 244 [2] G. Diambri-Palazz *et al.* Phys. Rev. Lett. **25**, 478 (1970); R. O. Avakyan *et al.*,  
245 Proc. High En. Phys. Conf. , Dubna **2** (1971); R. Schwitters, SLAC-TN-70-032;  
246 W. Kaune *et al.*, Phys. Rev. D **11**, 478 (1975); A. Jackson, Nucl. Instrum. Meth.  
247 **129**, 73 (1975); R. Brockmann *et al.*, BONN-IR-79-25 (1979); F. Rambo *et al.*,  
248 Phys. Rev. C **58**, 489 (1998); D. Lohmann *et al.*, Nucl. Instrum. Meth. A **343**, 494  
249 (1994).
- 250 [3] D. I. Sober *et al.*, Nucl.Inst.and Meth. A, 440 (2000),p.263.

- 251 [4] ELJEN Technology Plastic Scintillators <http://www.eljentechnology.com>.
- 252 [5] F. Barbosa *et al.*, Proceedings of IEEE Nuclear Science Symposium, Hawaii,  
253 USA (2007).
- 254 [6] F. Barbosa *et al.*, Proceedings of IEEE Nuclear Science Symposium, Virginia,  
255 USA (2002).
- 256 [7] Hamamatsu Corporation, MPPC S10931-050P, [http://www.](http://www.electronicdatasheets.com/pdf-datasheets/hamamatsu/s10931050p)  
257 [electronicdatasheets.com/pdf-datasheets/hamamatsu/s10931050p](http://www.electronicdatasheets.com/pdf-datasheets/hamamatsu/s10931050p).
- 258 [8] P. Eckert, H. C. Schultz-Coulon, W. Shen, R. Stamen and A. Tadday, Nucl. In-  
259 strument. Meth. A **620**, 217 (2010).

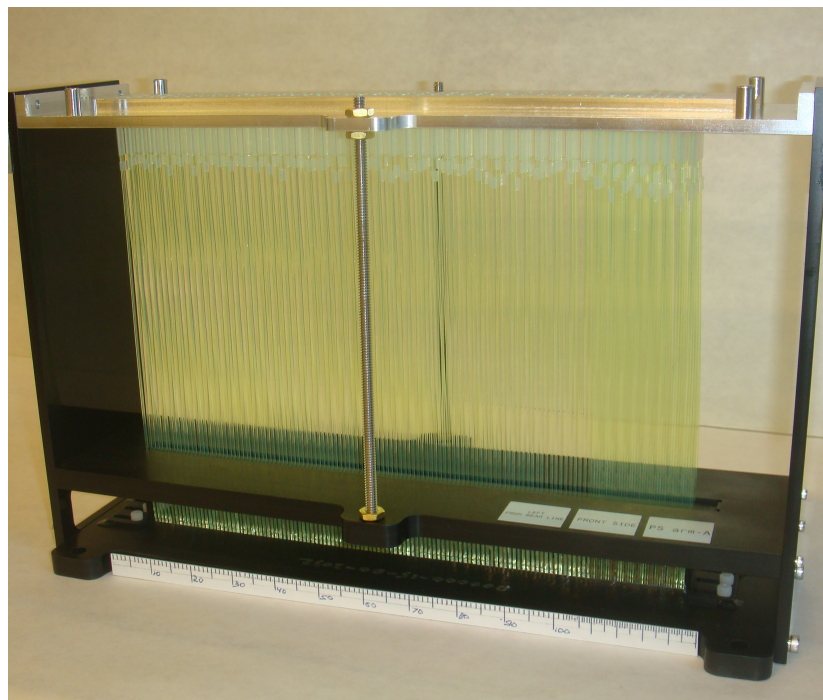
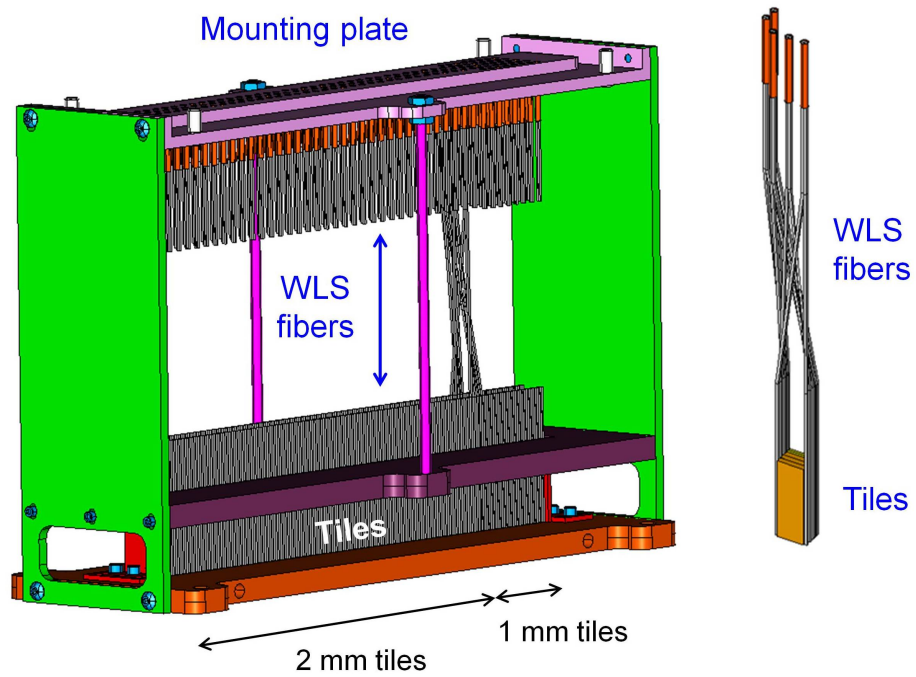


Figure 2: Schematic view of the pair spectrometer hodoscope (top). Light from scintillator tiles is collected using WLS fibers, which are inserted into holes in the mounting plate. Fabricated detector is shown in the bottom picture.

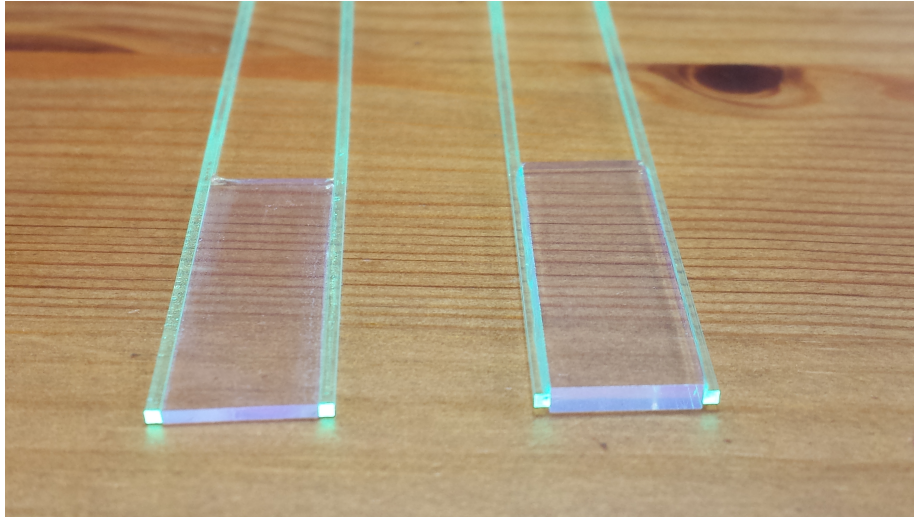


Figure 3: Scintillator tiles with two WLS fibers glued to sides of each tile: 3 cm x 1 cm x 1 mm tile (left) and 3 cm x 1 cm x 2 mm tile (right).

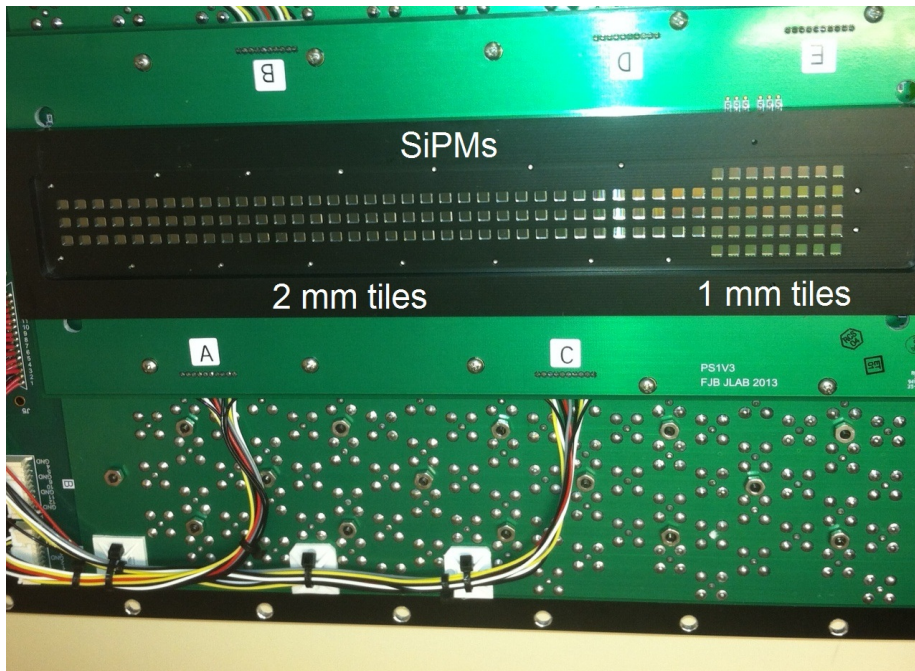


Figure 4: Electronics board with 145 silicon photomultipliers.

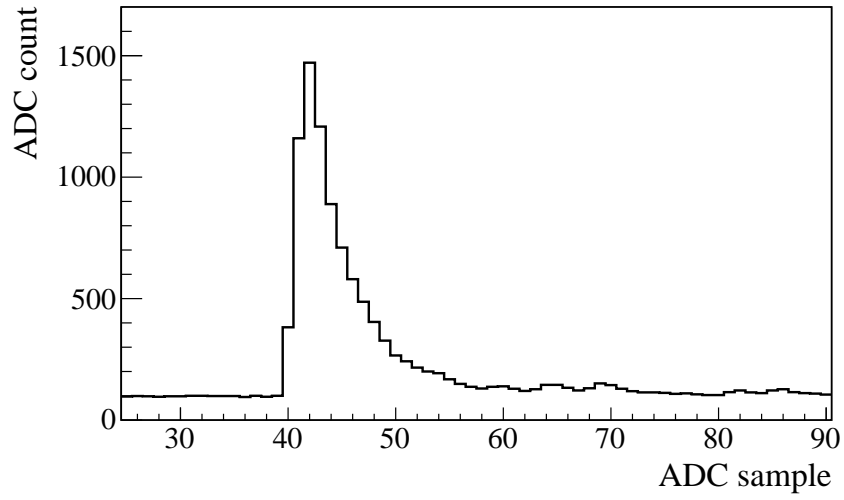


Figure 5: A typical flash ADC signal pulse obtained from a scintillator tile.

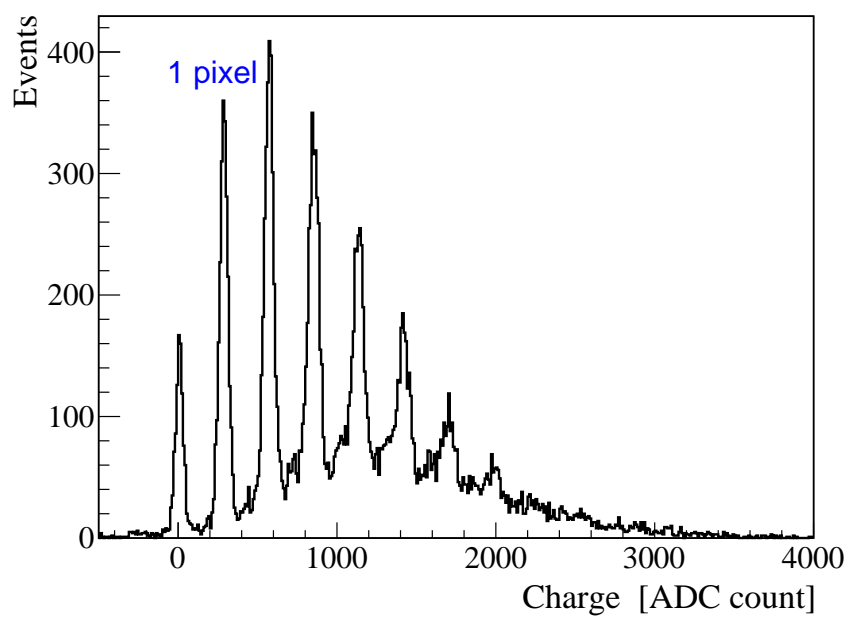


Figure 6: An example of the ADC spectrum obtained from SiPMs during electronics tests using a laser pulser. The first peak on the spectrum around ADC count zero corresponds to the ADC pedestal.

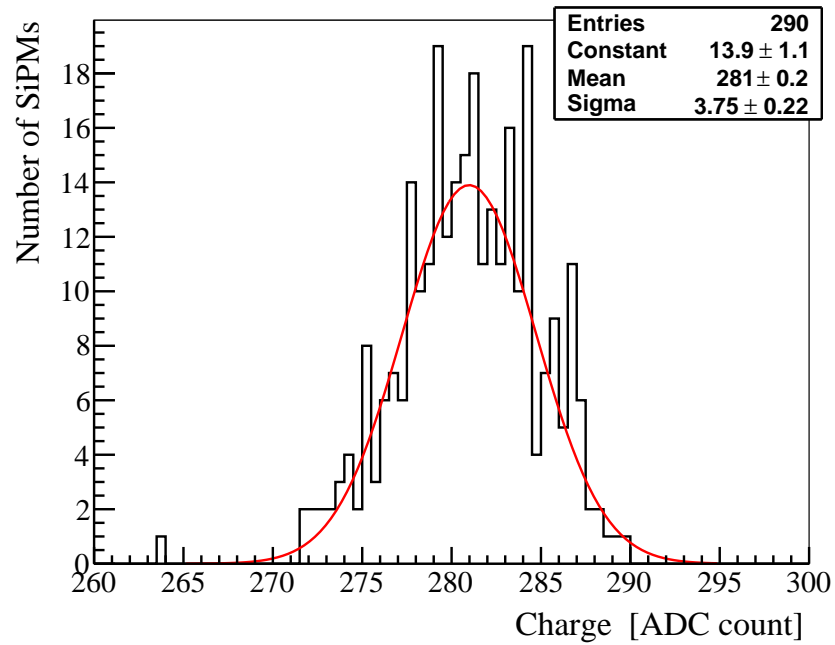


Figure 7: Distribution of the single-pixel peak measured by flash ADC for 290 hodoscope channels.

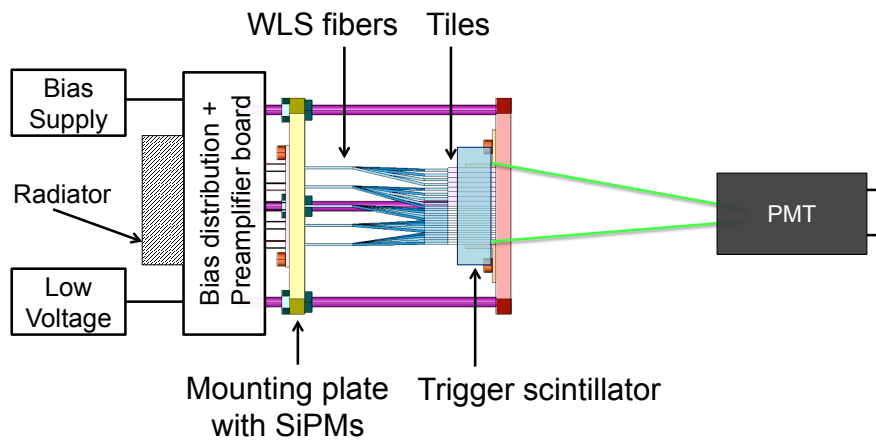


Figure 8: Top view of the hodoscope prototype with the trigger scintillator used in the beam test in experimental Hall B.



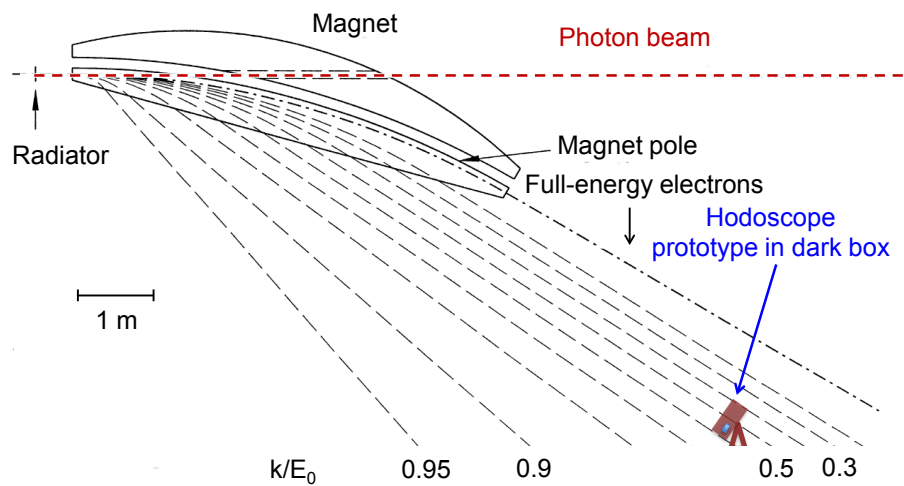


Figure 9: Hall B tagger system. Location of the hodoscope prototype under the Hall B tagger. Dashed curves denote trajectories of tagged electrons.

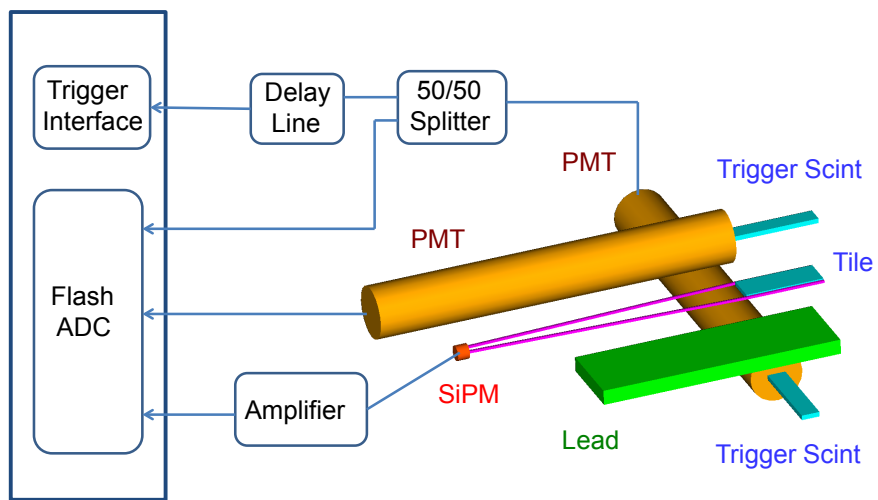


Figure 10: A cosmic ray setup.

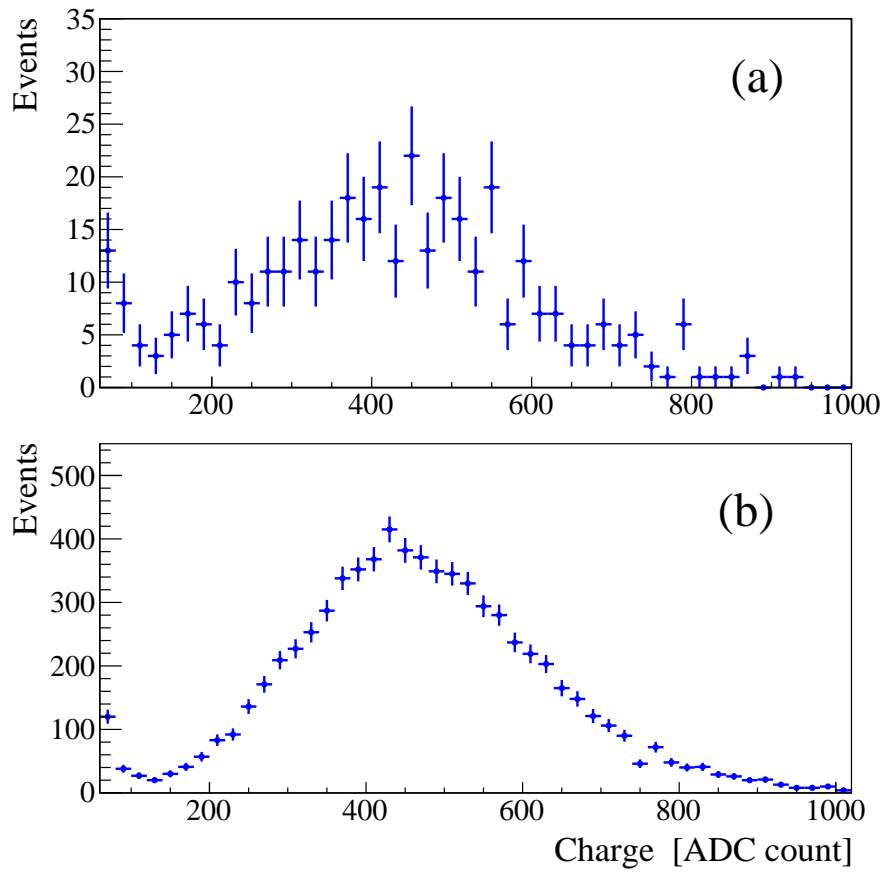


Figure 11: ADC spectra for a 2 mm wide tile measured with cosmic muons (a) and a  $^{90}\text{Sr}$  radioactive source (b).